

Linearization of F-I Curves by Adaptation

Bard Ermentrout

Department of Mathematics, University of Pittsburgh, Pittsburgh, PA 15260, U.S.A.

We show that negative feedback to highly nonlinear frequency-current (F-I) curves results in an effective linearization. (By *highly nonlinear* we mean that the slope at threshold is infinite or very steep.) We then apply this to a specific model for spiking neurons and show that the details of the adaptation mechanism do not affect the results. The crucial points are that the adaptation is slow compared to other processes and the unadapted F-I curve is highly nonlinear.

1 Introduction ---

Many computational models of neural networks use a simple threshold-linear output function for the firing rate, primarily for ease of analysis (Salinas & Abbott, 1996; Ben-Yishai, Hansel, & Sompolinsky, 1997, for example). This type of firing rate function can be a good approximation to regular spiking cells in sensory cortex (Mason & Larkman, 1990; Avoli & Olivier, 1989; McCormick, Connors, Lighthall, & Prince, 1985; Stafstrom, Schwindt, & Crill, 1984). Unlike fast spiking cells, regular spiking cells show adaptation to inputs. (Compare Figures 1 and 6 in McCormick et al., 1985.) The initial firing rate is fast and then slows to a steady-state rate. The curves of steady-state firing as a function of the input current (F-I curves) are very close to linear, whereas the initial interspike interval (an approximation of the firing rate before adaptation) is quite nonlinear. Wang (1998) has recently described a model for adaptation and, exploiting the fact that the adaptation process is slow, derives the firing rate and many other properties of adaptation. He uses a model for adaptation based on a calcium-dependent potassium channel (see below). He first considers the model without adaptation and fits the steady-state calcium concentration to a straight line. He then uses this to derive a firing rate for the adaptation, which is linear. This last fact is not surprising since his approximation for calcium concentration is also linear. Our goal here is to show that the F-I curve is linearized in *any* model with slow adaptation, provided that the unadapted firing rate curve is sufficiently *nonlinear*. The latter condition occurs in simple models such as the integrate-and-fire neuron, as well as in more “realistic” models such as Traub’s Hodgkin-Huxley-type model for spiking dynamics. That is, we make no a priori approximations; the linearization is a consequence of the analysis, not an assumption. We derive a similar model to Wang’s

“calcium” model but exploit the full nonlinear aspects of the F-I curve in our subsequent analysis. We close with some specific examples.

2 Negative Feedback and Linearization

We start with an abstract model. Suppose that in the absence of negative feedback, the firing rate curve is given by a function, $f(I)$, and we can suppose that the threshold current for firing is $I = 0$ by shifting the threshold. Then $f(I) = 0$ if $I < 0$ and $f(I)$ is continuous for $I \geq 0$. This last condition says that the firing rate must tend to zero as the current tends to zero. The Hodgkin-Huxley model does not have this property since the firing rate is some nonzero value as soon as the threshold is crossed (see Rinzel & Ermentrout, 1989). The integrate-and-fire model has a firing rate given by

$$f_{iar}(I) = \frac{K_1}{\log(1 + K_2/I)},$$

which does vanish as $I \rightarrow 0$. The firing rate for many cortical models, including the Traub model, is well approximated by

$$f_{sn}(I) = A\sqrt{I}. \quad (2.1)$$

Both of these firing rates are highly nonlinear in that they cannot be approximated by a linear function near threshold. In both cases, the derivative of the function tends to infinity as the current decreases to threshold. Now suppose that there is negative feedback, due to adaptation, which slows the firing rate. Let z be the amount of this negative feedback so that the true firing rate is $f(I - gz)$. The parameter g is the degree of negative feedback. This feedback term is in turn proportional to the firing rate so that

$$z = \beta f(I - gz). \quad (2.2)$$

(This is not an unreasonable assumption, as we will see below in the analysis of biophysical models.) We must solve this for z and then use the result to obtain the true firing rate. Note that if $I = 0$, then $z = 0$ and there is no adaptive feedback. To see that firing rate will be linearized, we implicitly differentiate this:

$$\frac{dz}{dI} = \beta f'(I - gz) \left(1 - g \frac{dz}{dI} \right),$$

hence,

$$\frac{dz}{dI} = \frac{\beta f'}{1 + \beta g f'}.$$

Our nonlinearity assumption implies that the derivative of f is very large when I is small, so that we must have

$$\frac{dz}{dI} = \frac{1}{g},$$

and from this we conclude that

$$z \approx \frac{I}{g}$$

and that the true firing rate,

$$F = \frac{z}{\beta} \approx \frac{I}{\beta g}.$$

Thus, the negative feedback makes the behavior of the steady-state firing rate linear with the injected current. Furthermore, the details of the firing rate function itself do not even contribute to the slope of this function at low inputs. Only the degree of adaptation and the proportionality of the adaptation to firing rate matter.

As a concrete example, suppose that the firing rate is like equation 2.1. Then we can solve for the true firing rate:

$$f_{\text{adapt}}(I) = \frac{-A^2 g \beta + \sqrt{(A^2 \beta g)^2 + 4A^2 I}}{2}. \quad (2.3)$$

Note that the slope of this function at $I = 0$ is $1/(g\beta)$, as noted in general in the above calculation.

3 Application to Biophysical Models ---

The typical biophysical model consists of several compartments and has the form,

$$C \frac{dV}{dt} = - \sum_k g_k(t) (E_k - V) + I, \quad (3.1)$$

for each compartment, and the time-dependent conductances have the form,

$$g_k(t) = \bar{g}_k m_k^p(t) h_k^q(t),$$

where the gates, m_k , h_k , obey first-order differential equations that are dependent on voltage or other quantities such as calcium. We want to separate out one of these conductances as having slow dynamics compared to all the others. This will represent the adaptation. Thus, we will write the sum in equation 3.1 as

$$-I_{\text{ion}} - \bar{g} z (V - E_{\text{adapt}}),$$

where

$$\frac{dz}{dt} = \epsilon Z(V, z, \dots),$$

and ϵ is a small, positive parameter. Now we make our main assumption about the dynamics of the fast subsystem. If $g = 0$ as the current increases, the dynamics makes a transition from rest to repetitive firing via a saddle-node bifurcation on a circle. This type of bifurcation occurs in most models of cortical neurons when there is no adaptation. Then, it is known (see Rinzel & Ermentrout, 1989; Ermentrout, 1994; Hoppensteadt & Izhikevich, 1997) that the firing rate near the critical current at which the transition is made is

$$f = A\sqrt{I - I_c}.$$

Thus, the square-root firing relation discussed in the previous section arises naturally from the dynamics.

In many neurophysiology articles, the F-I curve is depicted as bilinear (cf. Stafstrom et al. 1984), with a steep slope at low currents and a shallower slope at high currents. This is exactly what one would expect with a square-root relationship. Figure 1A shows the data from their article together with the square-root F-I curve. (The points on this graph were obtained by digitizing their figure of the first interspike interval for cat layer V neurons during current injection. The first interspike interval presumably reflects the instantaneous firing rate before adaptation turns on.)

Now we turn to the slow dynamics of the adaptation. We write the dynamics as

$$\frac{dz}{dt} = \epsilon(H(V, \dots) - z),$$

where H depends only on the “fast” equations. When there is no firing, we assume that H is very close to zero so the adaptation does not contribute much hyperpolarization at rest. When firing repetitively, the potential and the other variables are periodic so that we can formally average the slow equation, obtaining

$$\frac{dz}{dt} = \epsilon\left(\frac{1}{T} \int_0^T H(V(t), \dots) dt - z\right).$$

Last, we suppose that the spike width does not vary much over a range of current; thus, the integral of H over one period of the oscillation is roughly a constant, say, β . Since $1/T$ is just the firing rate, f , we see that

$$\frac{dz}{dt} \approx \epsilon(\beta f - z).$$

Finally, the firing rate is proportional to the input current and the total outward current due to the adaptation. Near the transition from rest to repetitive firing, the potential spends most of the time near rest, so we can approximate the adaptation current by

$$I_{adapt} \approx \bar{g}z(V_{rest} - E_{adapt}) \equiv \bar{g}z\Delta. \quad (3.2)$$

We thus obtain the simple model for adaptation:

$$\frac{dz}{dt} = \epsilon(\beta A\sqrt{I - I_c - \bar{g}\Delta z - z}). \quad (3.3)$$

This allows us to model adaptation quantitatively because each of these parameters is readily computed. Only A , β require us to compute numerically the actual solutions as a function of the input; all other parameters are readily available from the model. Wang (1998) has noted that the sequence of interspike intervals can be fitted to an exponential function and has used his simple linear equation to derive the time constant. Equation 3.3 is not linear, so the approach to steady state is not so readily computed. However, empirically, we find that β is small, so that z will be quite small as long as βA is small compared to $g\Delta$, and we get the linear approximation

$$\frac{dz}{dt} = \epsilon\beta A\sqrt{I - I_c} - \epsilon\left(1 + \frac{\beta Ag\Delta}{2\sqrt{I - I_c}}\right)z.$$

The effective time constant is thus

$$1/\tau_{adapt} = \epsilon\left(1 + \frac{\beta Ag\Delta}{2\sqrt{I - I_c}}\right). \quad (3.4)$$

As Wang notes, the actual time constant for adaptation is faster than the time constant of the slow adaptation process. In fact, near threshold, the time constant can be quite small.

4 Examples

4.1 Traub Model with an M Current. We first consider Traub's model for spiking dynamics (Traub & Miles, 1991) with a slow outward potassium current. The equations are 3.1 where the fast current is:

$$I_{ion} = g_{Na}hm^3(V - E_{Na}) + g_L(V - E_L) + g_Kn^4(V - E_K).$$

The gating variables, m , h , n , obey equations of the form:

$$\frac{dy}{dt} = a_y(V)(1 - y) - b_y(V)y.$$

We used $a_m(V) = .32(54 + V)/(1 - \exp(-(V + 54)/4))$, $b_m(V) = .28(V + 27)/(\exp((V + 27)/5) - 1)$, $a_h(V) = .128 \exp(-(50 + V)/18)$, $b_h(V) = 4/(1 + \exp(-(V + 27)/5))$, $a_n(V) = .032(V + 52)/(1 - \exp(-(V + 52)/5))$, and $b_n(V) = .5 \exp(-(57 + V)/40)$. The other parameters are $C = 1 \mu\text{F}/\text{cm}^2$, $g_{Na} = 100$, $g_K = 80$, $g_L = .1 \text{ mS}/\text{cm}^2$, and $E_{Na} = 50$, $E_L = -67$, $E_K = -100 \text{ mV}$.

With these parameters, the critical current for the onset of rhythmicity is $0.45 \mu\text{A}/\text{cm}^2$. We find (see Figure 1B) that a good fit for the unadapted firing rate is

$$f(I) \approx 60\sqrt{I - I_c},$$

which is accurate except at high firing rates, where it is a little low. (The reason is that at high currents, the unadapted firing rate actually becomes more linear.)

We add adaptation via the current:

$$I_{\text{adapt}} = gz(V - E_K),$$

where,

$$\frac{dz}{dt} = 0.01(1/(1 + \exp(-(V + 20)/5)) - z).$$

In Figure 2A, we show the result of the adaptation when a current pulse of $5 \mu\text{A}/\text{cm}^2$ is injected and $g = 5 \text{ mS}/\text{cm}^2$. The initial firing rate is about 125 Hz and the steady-state firing rate is about 50 Hz. A numerical calculation shows that the average magnitude of the adaptation is proportional to the firing rate with factor, $\beta = 0.00045$. Using equation 2.3 along with equation 3.2 we get an approximation for the steady-state firing rate when there is adaptation. In Figure 1C, we plot the steady-state firing rate along with the computed firing rate from these two formulas. The fit is very good even though the nonadaptive firing rate approximation was somewhat low at high rates of firing. Figure 2B shows the slow variable z for the full model, as well as the solution to equation 3.3 with the parameters as chosen above. The dynamics is captured very closely. As with Wang's simulations, random inputs into the model are very nicely reproduced with the averaged model even though the inputs occur at a fast time scale. Equation 3.4 shows that for current near criticality, the time constant is quite small, so the system can respond quickly.

4.2 Calcium-Dependent Potassium Current. A more likely type of adaptation is one that arises from a calcium-dependent potassium current. We have computed this model as well. The fast ionic current is as above, with the addition of a high-threshold calcium current:

$$I_{Ca} = g_{Ca}m_{\infty}(V)(V - E_{Ca}),$$

where $m_{\infty}(V) = 1/(1 + \exp(-(v + 25)/5))$, $E_{Ca} = 120 \text{ mV}$, and $g_{Ca} = 1 \text{ mS}/\text{cm}^2$. Calcium obeys the dynamics

$$\frac{d[\text{Ca}^{2+}]}{dt} = -.002I_{Ca} - .0125[\text{Ca}^{2+}],$$

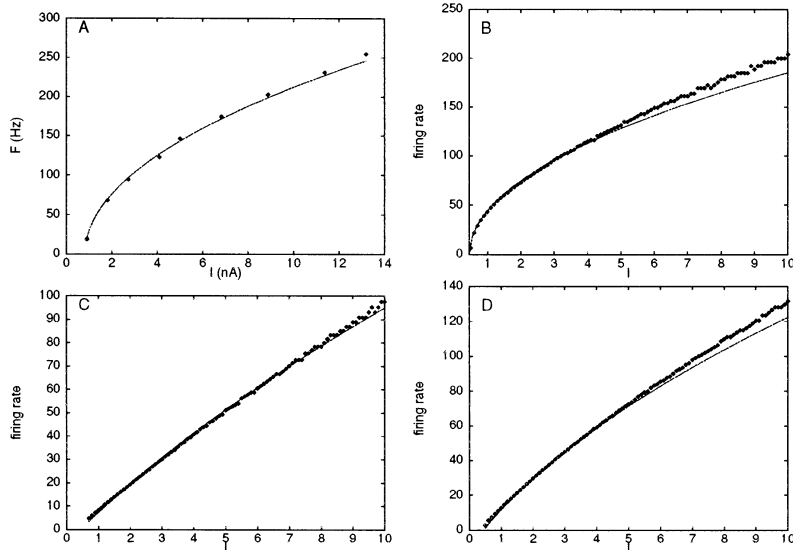


Figure 1: F-I curves for real cells and for models of cells computed numerically along with analytical functions obtained by averaging. (A) F-I curve from Stafstrom et al. (1984) fitted by the square-root function. (B) Traub model with no adaptation is well fitted by a square-root function. (C) Traub model with slow voltage-dependent potassium current with conductance, $g = 5 \text{ mS/cm}^2$, and the analytic approximation based on equation 2.3. (D) Calcium-based model with a calcium-dependent potassium current, $g_{ahp} = 5 \text{ mS/cm}^2$ and the analytic approximation. In curves B, C, and D, current is in $\mu\text{A/cm}^2$.

and the adaptive current is

$$I_{ahp} = g_{ahp}([Ca^{2+}]/(30 + [Ca^{2+}]))(V - E_K).$$

Here, the calcium concentration is the slow parameter. The same type of calculation above shows that the average calcium concentration in the absence of adaptation is a factor of $\beta = .008$ times the firing rate. The unadapted firing rate is about the same as the firing rate for our previous model. Figure 1D shows a plot of the steady-state firing rate for this model for $g_{ahp} = 5 \text{ mS/cm}^2$ using $A = 60$, $\beta = 0.008$ and approximating the nonlinear gate, $([Ca^{2+}]/(30 + [Ca^{2+}]))$ by $[Ca^{2+}]/30$ since the calcium concentration stays well below 30. As in the simpler adaptation model, the approximation of the steady-state firing rate fits the computed one very well.

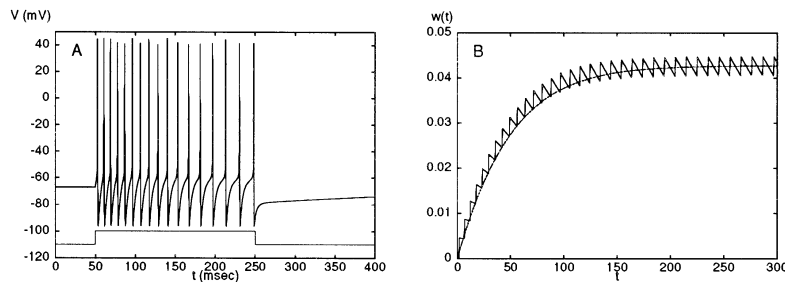


Figure 2: Response of the Traub model to a current pulse showing adaptation of the firing rate. (A) Voltage. (B) The adaptation gating variable for the full model using a voltage-dependent potassium current along with a solution to the averaged equation (3.3).

5 Discussion

We have derived a model for adaptation similar to that derived by Wang (1998). However, we have used no approximations that do not arise directly from formal analysis of the dynamics. In particular, we have not approximated the amount of adaptation by any ad hoc functions but rather obtained the approximations from the behavior of systems near a saddle-node limit cycle bifurcation. We have used a simple negative feedback argument to show that adaptation always linearizes nonlinear firing rates that are very steep near the transition to repetitive firing.

There are some intrinsic heuristics in our simplification. The square-root form of the firing rate is formally exact only in the neighborhood of the saddle-node bifurcation. However, in that neighborhood, the frequency of the oscillation is very small, so that in order to average the equations formally to get equation 3.3, the adaptation would have to be unrealistically slow. Thus, we have used the square root formula for the firing rate beyond the regime where it is formally correct. The result is that we have a model for linearization that is not valid right at the bifurcation or valid far from the bifurcation, but rather at some intermediate range. Nevertheless, the numerical calculations show that the formula is good over a far greater range than would be expected from a formal mathematical point of view.

Most neurons are better modeled by multiple compartments. In this case, there will be additional slow variables, and the simple scalar model (see equation 3.3) will not be valid. Instead, we will obtain equations for the

form:

$$\frac{dz_i}{dt} = \epsilon(\beta_i \sqrt{I - I_c - \sum_j g_{ij}z_j} - z_i),$$

where β_i and g_{ij} are related to how the adaptation in different compartments affects the somatic potential. Here we assume that only the soma is able to spike. The analysis of these equations is not as straightforward and would certainly depend on the number and strength of coupling between compartments.

Acknowledgments

This work was supported in part by the National Science Foundation and the National Institute of Mental Health.

References

- Avoli, M., & Olivier, A. (1989). Electrophysiological properties and synaptic responses in the deep layers of the human epileptogenic neocortex in vitro. *J. Neurophysiol.*, *61*, 589–606.
- Ben-Yishai, R., Hansel, D., & Sompolinsky, H. (1997). Traveling waves and the processing of weakly tuned inputs in cortical models. *J. Comput. Neuro.*, *4*, 57–77.
- Ermentrout, G. B. (1994). Reduction of conductance-based models with slow synapses to neural nets. *Neural Comp.*, *6*, 679–695.
- Hoppensteadt, F., & Izhikevich, E. (1997). *Weakly connected neural nets*. Berlin: Springer-Verlag.
- Mason, A., & Larkman, A. (1990). Correlation between morphology and electrophysiology of pyramidal neurons in slices of rat visual cortex, II. Electrophysiology. *J. Neurosci.*, *10*, 1415–1428.
- McCormick, D. A., Connors, B. W., Lighthall, J. W., & Prince, D. A. (1985). Comparative electrophysiology of pyramidal and sparsely spiny stellate neurons in the neocortex. *J. Neurophysiol.*, *54*, 782–806.
- Rinzel, J. M., & Ermentrout, G. B. (1989). Analysis of neuronal excitability. In C. Koch & I. Segev (Eds.), *Methods in neuronal modeling* (pp. 135–170). Cambridge, MA: MIT Press.
- Salinas, E., & Abbott, L. F. (1996). A model of multiplicative neural responses in parietal cortex. *PNAS(USA)*, *93*, 11956–11961.
- Stafstrom, C. E., Schwindt P. C., & Crill, W. E. (1984). Repetitive firing in layer V neurons from cat neocortex in vitro. *J. Neurophysiol.*, *52*, 264–277.
- Traub, R. D., & Miles, R. (1991). *Neuronal networks of the hippocampus*. Cambridge: Cambridge University Press.
- Wang, X. J. (1998). Calcium coding and adaptive temporal computation in cortical pyramidal neurons. *J. Neurophys.*, *79*, 1549–1566.

Received November 14, 1997; accepted February 23, 1998.